Dynamic Analysis of Beam with A Breathing Crack

S. Suresha,
Assistant Professor
School of Mechanical Engineering
Reva University Bangalore

D. Mallikarjuna Reddy,
Associate Professor
Department of Mechanical Engineering
Reva Institute of Technology and Mgmt, Bangalore

Abstract **—The importance of the beam and its engineering applications plays vital role in analysis, due to different types of loading on the beam. Since many types of loading on the beam causes various types of cracks. The occurred cracks and their locations effect on the shape and values of the beam frequency. Recently various types of crack analysis are prevailing in the industry of spacecraft, airplanes, wind turbines, turbines, robot arm and many other relevant field. In particular breathing crack is considered: the natural frequencies and mode shapes of beam with crack can provide an insight into the extent of damage.**

An attempt is been made to address the problem of vibrations of a Euler-Bernoulli beam with breathing crack. This phenomenon can be attributed to the presence of the non-linearity due to the opening and closing of cracks. In order better to understand the essential non-linear dynamics of the beam with crack, a bilinear two-degree-of-freedom model is studied. Also numerical study has been carried out to predict spectral pattern and the magnitude of each harmonic component for a simply supported beam containing breathing crack.

Keywords — Crack, Galerkin procedure, Non-linearity, Natural frequency, Bilinear

1. INTRODUCTION

The use of simplified models to simulate the nonlinear behavior of a real system has been a very challenging task in mechanics. Because of their simplicity, oscillators with bilinear or piecewise stiffness characteristics (i.e. with a bilinear or piecewise restoring forcing function) have been used to model the mechanical systems with nonlinear stiffness. For example,

1. Modeled cantilever beams with nonlinear boundary conditions by oscillation with bilinear stiffness.
2. Bearing suspension of high-speed rotors by oscillators with piecewise stiffness.
3. To model the nonlinearity of a wave-driven off-shore tower.
4. To model the nonlinear elastic supports of a rigid rotors.
5. To simulate the behavior of print hammers. [1]

The use of bilinear oscillators can be used to model the dynamic behavior of structures with a fatigue crack [2]. A breathing crack was introduced based on the bilinear stiffness concept, which assumes that the opens (with lower crack stiffness) or closes (with higher stiffness) depending on the direction of the vibration. [4, 5, 13]
Since all numerical simulation techniques require tremendous computational time during the analysis. The advantage of using stiffness modeling technique is that both the homogeneous solution and the particular solution can be expressed in terms of two square wave functions.

The construction of supersonic aircraft structures and high-speed rotating machines such as steam turbines, generators, motors and pumps, etc., has become more complicated since the late 1950s. Although these machines are carefully designed for fatigue loading, possess high levels of safety, are constructed with high-quality materials, and are thoroughly inspected prior to service as well as periodically during their operating lives, still there are instances of cracks or damage escaping inspection. Therefore, the development of the structural integrity monitoring techniques has received increasing attention in recent years. Among these monitoring techniques, it is believed that the monitoring of the global dynamics of a structure offers favorable alternative if the on-line (in service) damage detection is necessary. [15]

In order to identify structural damage from vibration monitoring, the study of the changes of the structural dynamic behavior due to cracks is required for developing the detection criterion. Some earlier research based on the open crack model, which assumes cracks always keep open during the vibration process, has been proposed.
The time histories of the vibrations showed the existence of the nonlinear behavior for structures with fatigue cracks. For example,

1. Modeling of the fatigue crack as a bilinear spring and using the bondgraph technique to analyze the first five modes of a cracked cantilever beam. [6,7]
2. A pair of self-equilibrating forces and piecewise stiffness to model the contact phenomenon of a crack during the longitudinal vibration. [10,11]

2. APPLICATION TO EULER - BERNOULLI BEAM WITH CRACK

The governing equation for beams with a fatigue crack obtained from the Galerkin procedure has not only bilinear stiffness but also bilinear forcing functions. The magnitude of the external excitation for each mode of vibration indeed changes with the stiffness constant. To analyze the

vibrations of Euler - Bernoulli beams, it is necessary to extend the stiffness modeling technique to incorporate the bilinear forcing function [8, 9]

We consider a Euler - Bernoulli beam of rectangular cross section of depth 2d and width, 2b with an edge crack of size a, located at $x = x_c$, is shown in Figure 2.1

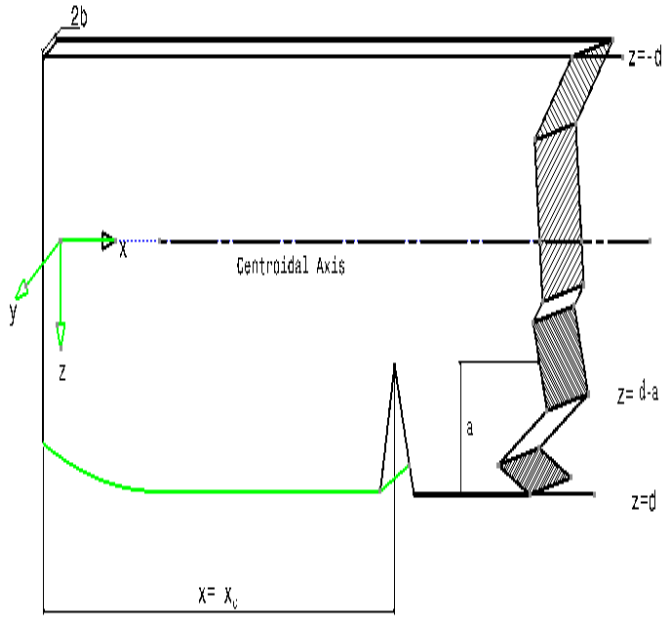

Fig 2.1 Configuration of the Euler - Bernoulli beam.

2.1 The equation of motion

$$I+\gamma(L_1-K-K_1)Q_1W''''+[2(I+\gamma[L_1-K-K_1])Q_1' +\gamma(2L_3+L_2-K_2+2K^1)Q_1]W''' +[(I+\gamma[L_1-K-K_1])Q_1''+\gamma(2L_3+L_2-K_2+2K')Q_1' +\gamma(L_4+L_5-K'')Q_1]W''+\rho A/E\,\ddot{W}=0 \quad (1)$$

where the functions

$I,\ K_1,\ K_2\ L,\ L_1,\ L_2,\ L_3,\ L_4,\ L_5 \wedge Q_1$

are defined as

$$L_2=\int_A d\varphi^1\,dA \qquad L_3=\int_A f^1\varphi\,dA$$

$$L_4=\int_A f^{11}\varphi\,dA \qquad L_5=\int_A f\varphi^1\,dA$$

$$Q_1=I+\gamma(L_1-K-K_1)/\,I+\gamma(L-2K) \quad (2)$$

External Excitation, F (x, t) is considered in Eq. 1, can be modified simply by adding a forcing function.

$$\frac{\rho A}{E}\times\ddot{W}+[I+\gamma(L_1-K-K_1)]Q_1W''''+\{2[I+\gamma(L_1-K-K_1)]Q_1' +\gamma(2L_3+L_2-K_2+2K')Q_1\}W''' +\{[I+\gamma(L_1-K-K_1)]Q_1'' +\gamma(2L_3+L_2-K_2+2K')Q_1'+(L_4+L_5-K'')Q_1\}W''=F(x,t)$$

transverse displacement is

$$W_i(x,t)=\gamma\psi_{ic}(x)u_i(t)+(1-\gamma)\psi_{inc}(x)u_i(t) \quad (3)$$

where ψ_{ic} is the i[th] mode shape of the cracked beam

ψ_{inc} is the i[th] mode shape of the uncracked beam

u_i is the general coordinate for each mode

To further simplify the problem, a harmonic forcing function is considered here, which is given as

$$F(x,t)=\xi(x)\sin\Omega t \quad [14] \quad (4)$$

Eqs. 3 and **4** into Eq. 2, we get

$$\{\gamma[r(x)\psi_i^{c''}+g(x)\psi_i^{c'}+h(x)\psi_i^{c}]+(1-\gamma)[r(x)\psi_i^{nc''}+g(x)\psi_i^{nc'}+h(x)\psi_i^{nc}]\}u_i+\frac{\rho A}{E}[\gamma\psi_i^{c}+(1-\gamma)\psi_i^{nc}]\ddot{u}_i=\xi(x)\sin\Omega t \quad (5)$$

where the functions

$r(x)\ g(x)\ and\ h(x)$ are given as

$$r(x)=[I+\gamma(L_1-K-K_1)]Q_1 \quad (6)$$

$$g(x)=2[I+\gamma(L_1-K-K_1)]Q_1'+\gamma(2L_3+L_2-K_2+2K')Q_1 \quad 7)$$

$$h(x)=(I+\gamma[L_1-K-K_1])Q_1''+\gamma(2L_3+L_2-K_2+2K')Q_1'+\gamma(L_4+L_5-K'')Q_1 \quad (8)$$

2.2 Calculation of the constant m

The stress (or strain) distribution is characterized by the crack function *f* with the parameters *α* and *m* defining stress profiles in the *x* and *z* directions. Since the stress along the *z* direction is assumed to be linear, its decay rate *m* can be estimated from the condition that the same bending moment is carried by the cracked beam and the uncracked beam at the crack. (3)

$$m=\frac{1}{1+\frac{3}{4}\left(\frac{a}{d}\right)^2-\frac{3}{2}\left(\frac{a}{d}\right)+\frac{1}{8}\left(\frac{a}{d}\right)^3}$$

3. RESULTS AND DISCUSSIONS

This gives the graphs of time history, spectrum of the forced response and system resonance in case of simply supported Euler-Bernoulli beam. These graphs are plotted using MATLAB codes are developed for generating the graphs as explained. Section 3 gives the history graph of simply supported Euler-Bernoulli beam with a forcing frequency of

3Hz and natural frequencies 28.7Hz and 26.5Hz. Remaining section give graph of spectrum of the system resonance and forced response in case of simply supported Euler-Bernoulli beam for the two forcing frequencies 8Hz and 3Hz.

$$u_f(t)=\frac{1}{2}\left(\frac{\mathrm{P}}{\omega_1^2-\Omega^2}+\frac{\mathrm{P}}{\omega_2^2-\Omega^2}\right)\sin\Omega t+\left(\frac{\mathrm{P}}{\omega_1^2-\Omega^2}-\frac{\mathrm{P}}{\omega_2^2-\Omega^2}\right)\left\{\frac{1}{\pi}-\frac{2}{\pi}\sum_{k=1}^{\infty}\frac{\cos 2k\,\Omega t}{(2k+1)(2k-1)}\right\} \quad (9)$$

$$u_s(t)=\frac{1}{2}[\mathrm{A}_1\sin\omega_1 t+\mathrm{A}_2\sin(\omega_2 t+\beta_0)]+\frac{\mathrm{A}_1}{\pi}\sum_{k=1,3,5}^{\infty}\frac{\cos(\omega_1-k\Omega)t-\cos(\omega_1+k\Omega)t}{k}-\frac{\mathrm{A}_2}{\pi}\sum_{k=1,3,5}^{\infty}\frac{\cos[(\omega_2-k\Omega)t+\beta_0]-\cos[(\omega_2+k\Omega)t+\beta_0]}{k} \quad (10)$$

$$u_f(t)=\frac{1}{2}\left(\frac{P_1}{\omega_1^2-\Omega^2}+\frac{P_2}{\omega_2^2-\Omega^2}\right)\sin\Omega t+\left(\frac{P_1}{\omega_1^2-\Omega^2}+\frac{P_2}{\omega_2^2-\Omega^2}\right)\left\{\frac{1}{\pi}-\frac{2}{\pi}\sum_{k=1}^{\infty}\frac{\cos 2k\,\Omega t}{(2k+1)(2k-1)}\right\} \quad (11)$$

$$u_s(t)=\frac{1}{2}\left[A_1\sin\omega_1 t+A_2\sin(\omega_2 t+\beta_0)\right]+\frac{A_1}{\pi}\sum_{k=1,3,5}^{\infty}\frac{\cos(\omega_1-k\Omega)t-\cos(\omega_1+k\Omega)t}{k}-\frac{A_2}{\pi}\sum_{k=1,3,5}^{\infty}\frac{\cos[(\omega_2-k\Omega)t+\beta_0]-\cos[(\omega_2+k\Omega t+\beta_0)]}{k} \quad (12)$$

3.1 Bilinear oscillator:

The time history of the bilinear oscillator is plotted by Eqs. 11 and 12 is shown in Fig 3.1. The positive peaks indicate the crack opening with amplitude varying from 0 to 2e-7. The negative peak is very small indicating crack closure. Same cycles get repeated after each interval of the 0.2 sec.

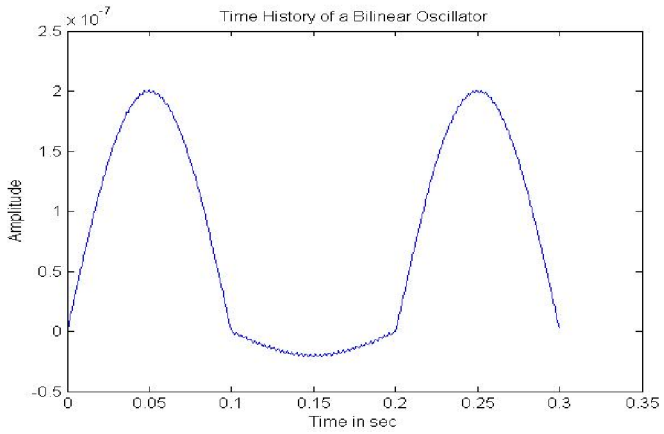

Fig. 3.1 Time history of a bilinear oscillator with Ω = 5 Hz, ω_1 = 355.9 Hz, ω_2 = 1125.4 Hz obtained from numerical simulation

3.2 Forced response of a bilinear oscillator

Spectrum of the bilinear oscillator under forced response is plotted by Eq. 9 is shown in Fig 3.2 The response consists of displacements indicated by the peaks. The amplitude decreases with increase in the frequency and after frequency range of 20 Hz it almost remains same since time required for crack opening is less

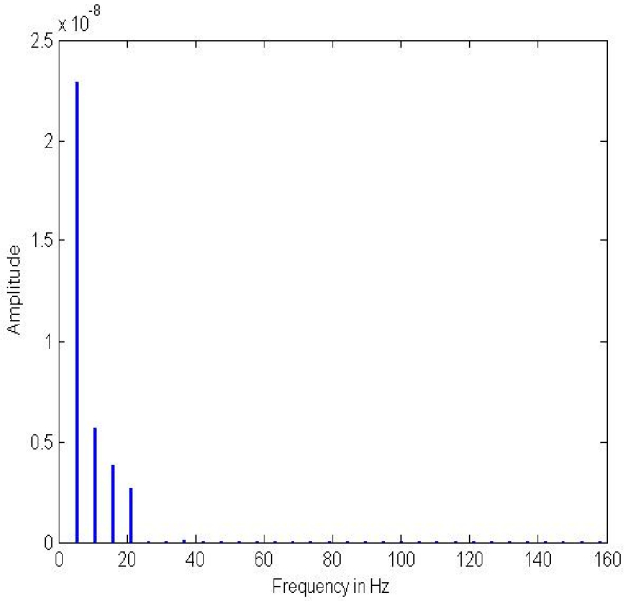

Fig.3.2 Spectrum of the forced response of a bilinear oscillator with Ω =8Hz, ω_1 =355.9Hz, ω_2 =1125.4Hz obtained from numerical simulation.

3.3. System resonance of a bilinear oscillator

Spectrum of the bilinear oscillator under system resonance is plotted by Eq.10 is shown in Fig 3.3 At system resonance the magnitude of amplitude is higher compared to forced response. Consider a case of the bilinear oscillator with Ω =8Hz ω_1 =355.9Hz, and ω_2 =1125.4Hz with forcing frequency Ω =8Hz. At lower frequency the amplitude starts increasing rapidly dominated by lower stiffness up to resonant frequency. After resonance the amplitude decreases due to lack of time for the crack to open sufficiently but at a lower rate. After resonant frequency range the amplitude is relatively zero.

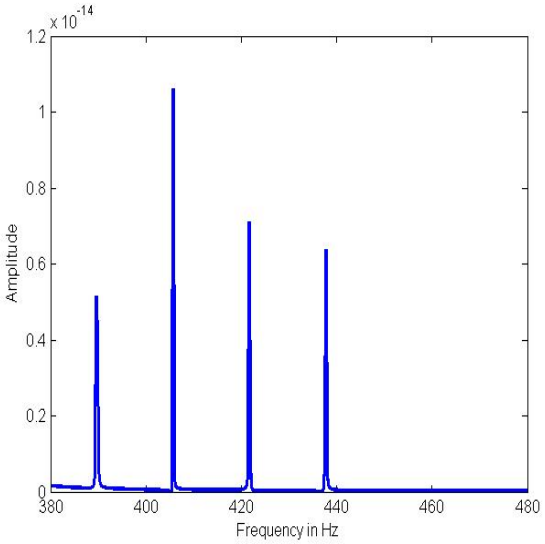

Fig.3.3 Spectrum of the system resonance of a bilinear oscillator for the frequency range of 380Hz to 480Hz obtained from numerical simulation.

3.4 System resonance of a bilinear oscillator

Spectrum of the bilinear oscillator under system resonance is plotted by Eq. 10 is shown in Fig 3.4 The change of frequency scale gives clear plot of amplitude with frequency scale magnified. Consider a case of the bilinear oscillator with Ω=8Hz ω_1=355.9Hz**,** and ω_2=1125.4Hz with forcing frequency Ω=8Hz. In this case amplitudes in the plots in Fig 3.4 has a increasing and decreasing behavior due to its different natural frequency.

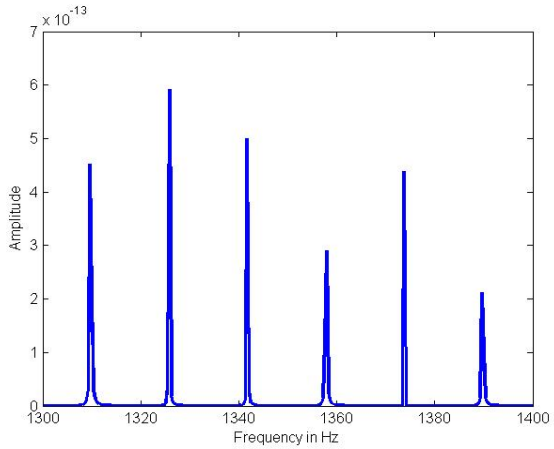

Fig. 3.4 Spectrum of the system resonance of a bilinear oscillator for the frequency range of 1300Hz to 1400Hz obtained from numerical simulation.

3.5 Simply supported Euler - Bernoulli beam

Time history for the first mode of vibration of a simply supported Euler - Bernoulli beam under the forcing frequency Ω=3Hz, ω_1=28.7Hz**,** and ω_2=26.5Hz**,** is plotted by Eqs. 11 and 12 are shown in Fig 3.5 The peaks are rough due to decreasing and increasing magnitude in small quantity since there is a varying lag of time between forcing and crack opening event.

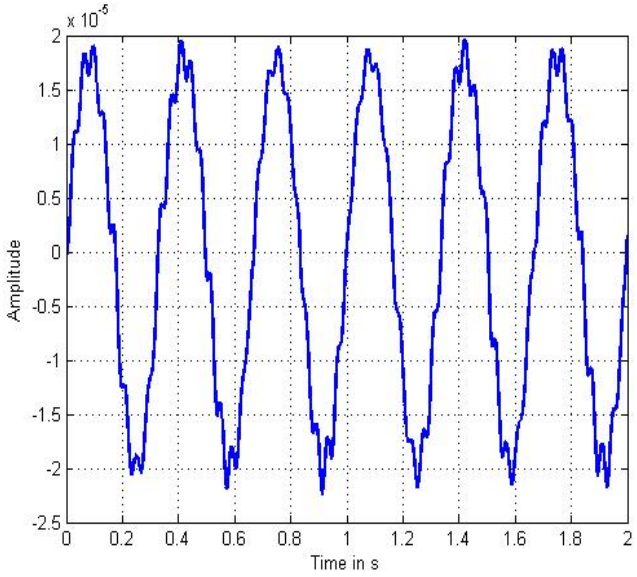

Fig. 3.5 Time history for the first mode of vibration of a simply supported Euler-Bernoulli beam under the forcing frequency Ω=3Hz, ω_1=28.7Hz, and ω_2=26.5Hz obtained from numerical simulation.

3.6 System resonance for the first mode of vibration of a simply supported Euler - Bernoulli beam

Spectrum of the simply supported Euler-Bernoulli beam under system resonance for the first mode of vibration is plotted by Eq.12 is shown in Figure 3.6 The simply supported Euler-Bernoulli beam case gives a plot with amplitudes changing even more rapidly. The amplitudes in the simply supported Euler-Bernoulli beam case is relatively more compared to bilinear oscillator. The amplitude starts from zero magnitude.

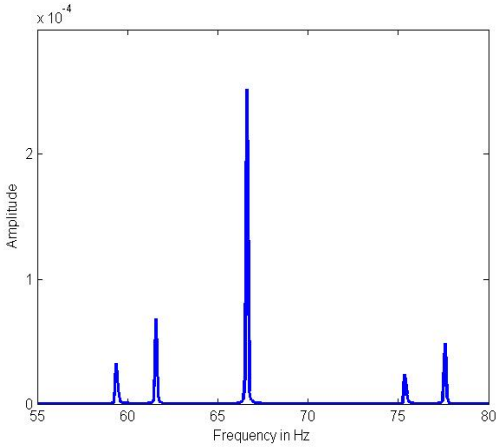

FIG. 3.6 Spectrum of the System resonance for the first mode of vibration of a simply supported Euler-Bernoulli beam under forcing frequency Ω=8Hz, ω_1=28.7Hz, ω_2=26.5Hz obtained from numerical simulation.

3.7 Forced response for the first mode of vibration of a simply supported Euler - Bernoulli beam

Spectrum of the simply supported Euler - Bernoulli beam under forced response for the first mode of vibration is plotted by Eq. 11 is shown in Fig 3.7 Consider the first mode

of vibration of a simply supported Euler - Bernoulli beam under forcing frequency Ω=8Hz, ω_1=28.7Hz and ω_2 =26.5Hz. For a forced response the starting amplitude is highest with all other amplitudes nearly zero since it is the weakest of all cases due to lack reaction moments.

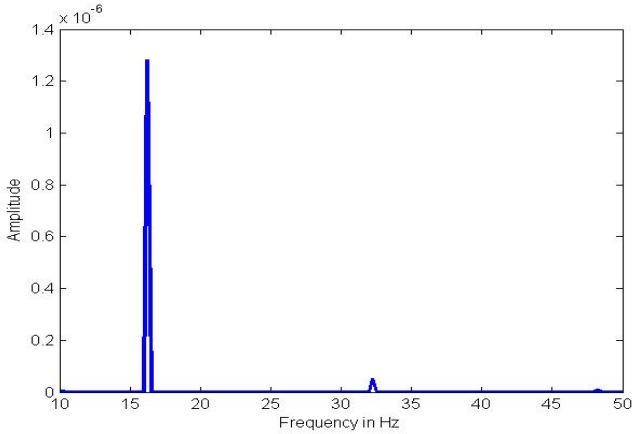

Fig. 3.7 Spectrum of Forced response for the first mode of vibration of a simply supported Euler-Bernoulli beam under forcing frequency Ω =8Hz, ω_1 =28.7Hz, ω_2 =26.5Hz obtained from numerical simulation

3.8 System resonance for the first mode of vibration of a simply supported Euler - Bernoulli beam

Spectrum of the simply supported Euler - Bernoulli beam under system resonance for the first mode of vibration is plotted by Eq. 12 is shown in Fig 3.8 Simply supported Euler - Bernoulli beam case is the weakest and do not yield amplitudes for higher frequencies. Thus if the forcing frequency is changed to Ω =3Hz from 8 Hz, and all other parameters are kept unaltered the resulting curve is shown in Fig 3.8 Amplitude here gives peaks with rapidly rising and falling magnitudes distributed over a frequency range.

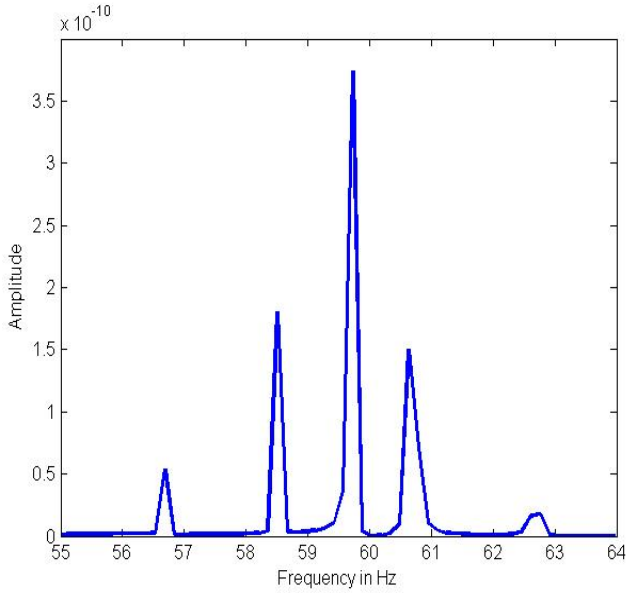

Fig. 3.8 Spectrum of system resonance for the first mode of vibration of a simply supported Euler - Bernoulli beam under the forcing Ω =3Hz, frequency ω_1 =28.7Hz, and ω_2 =26.5 Hz obtained from numerical simulation

3.9 Forced response for the first mode of vibration of a simply supported Euler - Bernoulli beam

Spectrum of the simply supported Euler - Bernoulli beam under forced response for the first mode of vibration is plotted by Eq. 11 is shown in Fig 3.9. To see the forced response the configuration of the previous case is kept unaltered except forcing frequency and simply supported Euler - Bernoulli beam case is simulated numerically

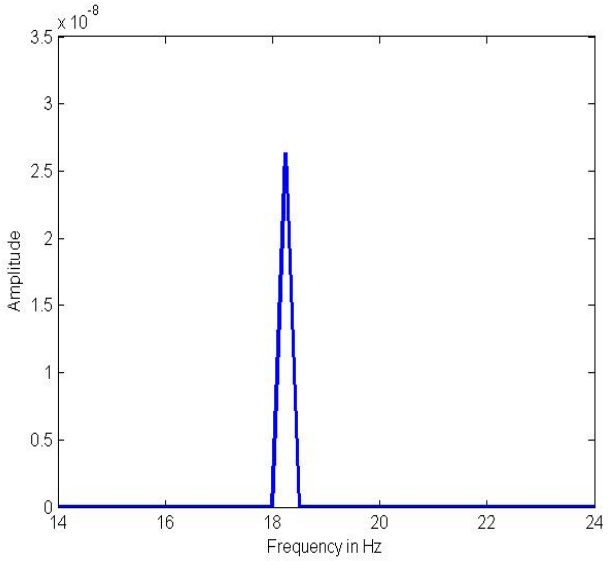

Fig. 3.9 Spectrum of forced response for the first mode of vibration of a simply supported Euler - Bernoulli beam under the forcing frequency Ω =3Hz, ω_1 =28.7Hz, and ω_2 =26.5Hz obtained from numerical simulation

4. CONCLUSIONS

The change of stiffness during free vibration using two square wave functions has been modeled and a closed-form solution for the forced vibration of a bilinear oscillator with constant-amplitude excitation has been studied. The occurred cracks and their locations effect on the shape and values of the beam frequency. An attempt is been made to address the problem of vibrations of a Euler-Bernoulli beam with breathing crack. Bilinear oscillator model is derived and checked for free and forced vibrations. The equations specifying spectral pattern for low frequency forced vibrations derived for both system resonance and forced response.

The derived equations are then applied to simulate a Euler - Bernoulli beam with external excitation. Parameter affecting the amplitude time response is completely known. The study yielded relations and time amplitude plot of a breathing crack which can be applied to find the crack growth in a structure subjected to fatigue.

5. REFERENCES

1. Y.C. Chu and M.H.H Shen, "*Analysis of Forced Bilinear Oscillators and the Application to Cracked Beam Dynamics*", AIAA Journal Vol.30, No.10, 1992, 2512-2519
2. Y.C. Chu and M.H.H Shen, "*Vibrations of Beams with a Fatigue Crack*", Computers and Structures Vol.45, No.1, 1992, pp. 79-93
3. Shen, M.H.H., and Pierre, "*Free Vibrations of beams with a Single-Edge Crack*", Journal of Sound and Vibration 170(2), (1994), 237-259.
4. E. Doukaa, L.J. Hadjileontiadisb "*Time–frequency analysis of the free vibration response of a beam with a breathing crack*", NDT&E International 38, 2005,3-10
5. A.D. Dimarogonas and J.Yao "*Vibration of a beam with a breathing crack*", Journal of sound& vibration 239(1), 2001, 57-67
6. S. Loutridisa, E. Doukab, L.J. Hadjileontiadisc "*Forced vibration behaviour and crack detection of cracked beams using instantaneous frequency*", NDT&E International 38, 2005, 411–419
7. E. Luzzato, "*Approximate computation of non-linear effects in a vibrating Cracked beam*", Journal of sound and vibration 265, 2003, 745–763
8. M. Chati, R. Rand and S.Mukherjee "*modal analysis of a cracked beam*", Journal of Sound and Vibration 207(2), 1997, 249-270
9. Jyoti K. Sinha, Michael I. Friswell "*Simulation of the dynamic response of a cracked beam*", Computers and Structures 80, 2002, 1473–1476
10. A.K. Darpe, K. Gupta, A. Chawla "*Coupled bending, longitudinal and Torsional vibrations of a cracked rotor*", Journal of Sound and Vibration 2002, 1-28
11. T.G. Chondros, A.D. Dimarogonas, J. Yao "*Longitudinal vibration of a bar with a breathing crack*", Engineering Fracture Mechanics 61, 1998, 503-518
12. S. M. Cheng, X.J.Wu and W.Wallace "*Vibrational response of a beam with a breathing crack*", Journal of Sound and vibration 225(1), 1999, 201-208
13. Nicola Pugno and Cecilla "*Evaluation of the Non- linear dynamic response to harmonic excitation of a beam with several breathing cracks*", Journal of Sound and Vibration 235(5) 2000, 749-762
14. W.T.Thomson, "*Theory of Vibration with Applications*", Third edition, 2002
15. Stanley T.Rolfe and John M. Barsom **"***Fracture and fatigue control in structures, Applications of Fracture Mechanics*", 1997 by Prentice-Hall, Inc. Englewood Cliffs, New Jersey 07632